Journal of Hydrology 563 (2018) 874–886

Contents lists available at ScienceDirect

Journal of Hydrology

journal homepage: www.elsevier.com/locate/jhydrol

Research papers

Effects of dynamic land use inputs on improvement of SWAT model performance and uncertainty analysis of outputs

Qingrui Wang, Ruimin Liu*, Cong Men, Lijia Guo, Yuexi Miao

State Key Laboratory of Water Environment Simulation, School of Environment, Beijing Normal University, No. 19, Xinjiekouwai Street, Beijing 100875, China

ARTICLE INFO

This manuscript was handled by G. Syme, Editor-in-Chief

Keywords:
Nonpoint source pollution
SWAT model
Climate change and human activity
Static and dynamic land use input
Uncertainty analysis

ABSTRACT

The objective of this study was to evaluate the impacts of static and dynamic land use input conditions on the performance of non-point source (NPS) model and find out whether dynamic land use input can improve the model accuracy. Soil and Water Assessment Tool (SWAT) model was selected as the evaluation model and seven different land use input conditions were set by setting the land use update file in SWAT. The results showed that the land use pattern in the study area changed from 2000 to 2015 due to climate change and human activities, leading to inconsistencies between different land use patterns. The calibrated results indicated that dynamic land use input conditions could apparently improve the simulation accuracy of total nitrogen (TN) and total phosphorus (TP). CE5Y condition had the best calibrated result with R^2 and NSE larger than 0.7 and 0.6, respectively. However, for flow simulation, the land use input conditions had no apparent effect on the model calibration and validation results. The deviation analysis of the model outputs indicated that monthly outputs were more affected by the land use input conditions than annual outputs and that deviations in wet seasons were larger than those in normal and dry seasons. The highest MAD occurred in June and August with a value of 82.87 t and 1.56 t for TN and TP, respectively. This study revealed the importance to consider the land use change when simulating the NPS pollution, and could provide support for land use input settings of NPS pollution models.

1. Introduction

Non-point source (NPS) pollution has been widely studied in recent years because it contains many uncertainties and is harder to control than point source pollution (Shen et al., 2015; Chen et al., 2017). Many studies have shown that NPS pollution has become the primary source of water contamination, rather than point source pollution (Wang et al., 2004; Mi et al., 2015). The simulation of NPS pollution should be carried out to provide information for its management. The mechanism models have been widely used to simulate NPS pollution with the development of computer science and the better understanding of the migration and transformation mechanism of pollutants in the real world (Moges et al., 2017; Yang et al., 2017a). The Soil and Water Assessment Tool (SWAT), the Annualized Agricultural Non-Point Source (AnnAGNPS) and the Hydrological Simulation Program – Fortran (HSPF) models have been used for the majority of NPS pollution simulations (Ahn and Kim, 2016; Karki et al., 2017; Teshager et al., 2017). Compared to the previously used export coefficient method and empirical models, the mechanism models have a higher simulation accuracy and universality (Liu et al., 2017b).

To appropriately control NPS pollution, the spatial and temporal characteristics of NPS pollution first need to be analyzed using models. The processes of NPS pollution generation and discharge are affected by many factors, such as land use type, topography, soil characteristics and meteorological conditions (Yang et al., 2017c; Lin et al., 2018; Zhi et al., 2018). These factors are also the basic input data for most NPS pollution models. Thus, the simulation results will be significantly affected by the spatial distribution and temporal changes in these input data (Bajracharya et al., 2018; Goyal et al., 2018). The spatial distribution data of these factors were used in most of the NPS models, considering the impacts of spatial variation of input data on the NPS pollution simulation (Du et al., 2016; Ouyang et al., 2016). In addition, the impacts of the spatial resolution of these input data on model outputs have also been analyzed by many studies (Kumar et al., 2017; Sun et al., 2017). However, for the temporal variations in NPS, only the time series of meteorological conditions were considered in most NPS models, while the other input data, such as land use type, topography and soil characteristics, were set as invariable during the simulation periods (Chen et al., 2013; Liu et al., 2013, 2014).

Analyzing the temporal characteristics of NPS pollution is conducive to the management of NPS contamination. Thus, the simulation periods of NPS pollution were usually long, from several years to several

* Corresponding author.
E-mail address: liurm@bnu.edu.cn (R. Liu).

https://doi.org/10.1016/j.jhydrol.2018.06.063
Received 19 April 2018; Received in revised form 21 June 2018; Accepted 24 June 2018
Available online 27 June 2018
0022-1694/ © 2018 Elsevier B.V. All rights reserved.

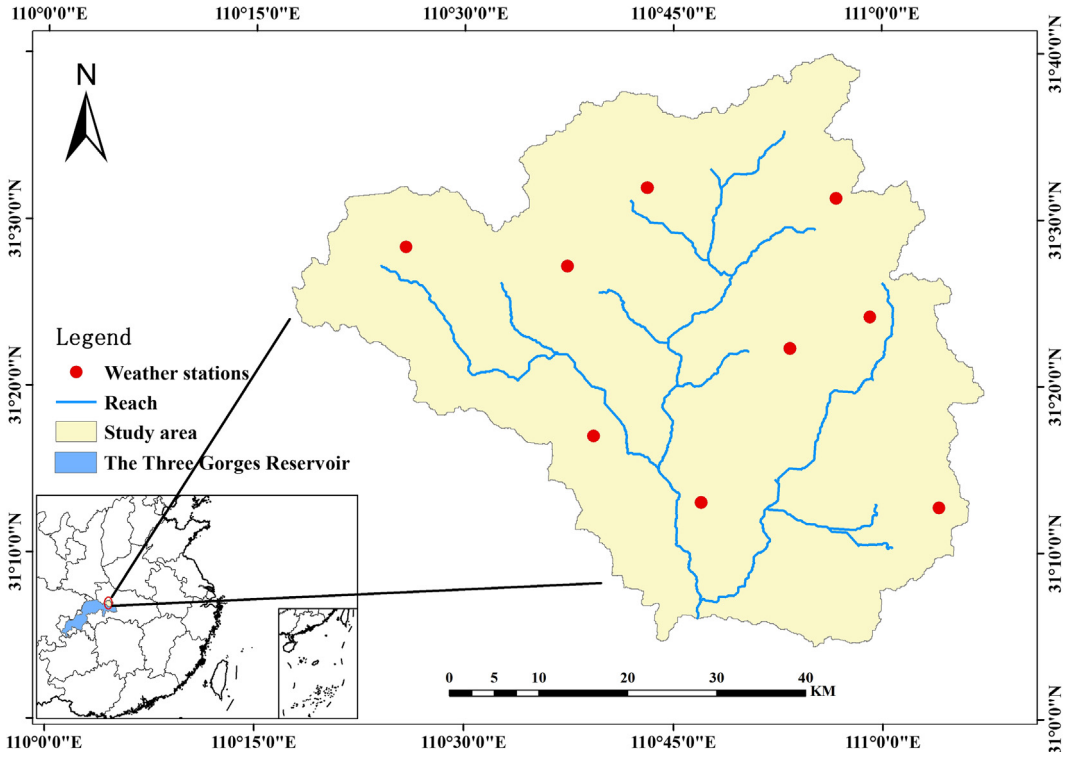

Fig. 1. Location of the Xiangxi River watershed.

decades, and simulation periods longer than 10 years were the most common (Ouyang et al., 2014; Zhai et al., 2014; Liu et al., 2017b). The temporal change of NPS pollution represents its response to changes in input data. Meteorological conditions experience the most change and have the greatest effects on the NPS pollution discharge within one year, but land use patterns will also change when the simulation periods are longer than several years. Many studies have found that land use will change significantly in 5 years (Sewnet and Abebe, 2017; Gashaw et al., 2018; Minta et al., 2018). When the time scale is large, in addition to meteorological conditions, the influence of land use change on the simulation of NPS pollution cannot be ignored.

The impacts of land use change on NPS pollution generation and discharge have received much focus in recent years (Chu et al., 2010; Zhang et al., 2013). In these studies, land use in different periods were used as input data to analyze the variations in model outputs resulting from land use change. However, land use in different periods was only set as different scenarios in these studies. In each simulation process, just one period of land use was used (Worku et al., 2017). These studies mainly focused on the influence of the spatial variations in land use patterns in different periods on NPS pollution, without taking temporal changes in land use into consideration. More recently, Wagner considered the land use dynamic change during SWAT simulation periods and found that different land use input scenarios during the period of simulation had great impacts on the SWAT model outputs (Wagner et al., 2017). This discovery embodied the temporal characteristics of land use change, but the analysis was only based on the predicted land use. The impacts of land use in different period on the temporal characteristics of NPS pollution need to be analyzed further.

In this study, the impacts of different land use input conditions on the model simulations were studied based on the SWAT model in Xiangxi river watershed. The main goals of this study were to (1) study the impacts of different land use input conditions on the model performance based on the calibration and validation results; (2) discuss whether dynamic land use input conditions can improve model performance; and (3) analyze the impacts of the land use input conditions on model outputs.

2. Materials and methods

2.1. Study area

The Xiangxi River is approximately 94 km long and is located between 110.47° to 111.13° E and 30.96° to 31.67° N in the Three Gorges Reservoir. It flows through three counties and its drainage area covers approximately 3099 km^2 (Fig. 1). The altitude in the area ranges from 110 m to 3088 m. A humid subtropical monsoon climate is the main climate in the watershed. The annual average precipitation is 1213.3 mm and the average annual temperature is 17.8 °C. June, July and August represent the wet season; April, May, September and October were the normal season; and January, February, March, November and December represent the dry season. Forest area dominates the total area of the watershed, with a proportion more than 80%. However, due to excessive fertilizer application and livestock breeding, the watershed still faces serious NPS pollution (Liu et al., 2016).

2.2. SWAT model and calibration

SWAT is a basin-scale, continuous-time model that was developed by the United States Department of Agriculture (USDA) Agricultural Research Service (ARS) (Arnold et al., 1998). The SWAT model is designed to simulate the impact of management on the hydrological processes and water quality (Kang et al., 2006). The SWAT model has been developed over 30 years. It is a descendant of the Simulator for Water Resources in Rural Basins (SWRRB) model (Arnold and Williams, 1987). To overcome the limitation that SWRRB can only simulate 10 subbasins at a time, the Routing Outputs to Outlet (ROTO) model was merged with SWRRB into the SWAT model (Arnold et al., 1995). The SWAT model simulates the hydrological process based on the water balance equation (Eq. (1)):

$$SW_t = SW_0 + \sum_{i=1}^{t} (R_{day} - Q_{surf} - E_a - W_{seep} - Q_{gw}) \quad (1)$$

where SW_t is the final moisture content of soil, SW_0 is the initial

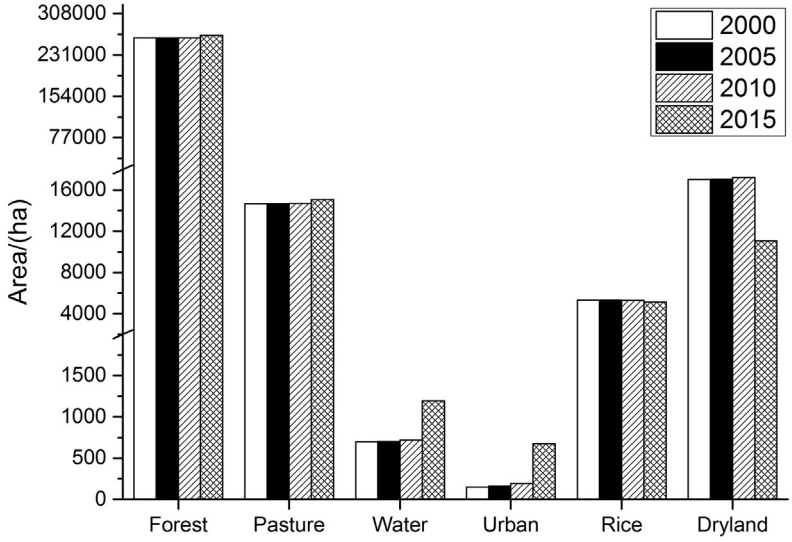

(a)

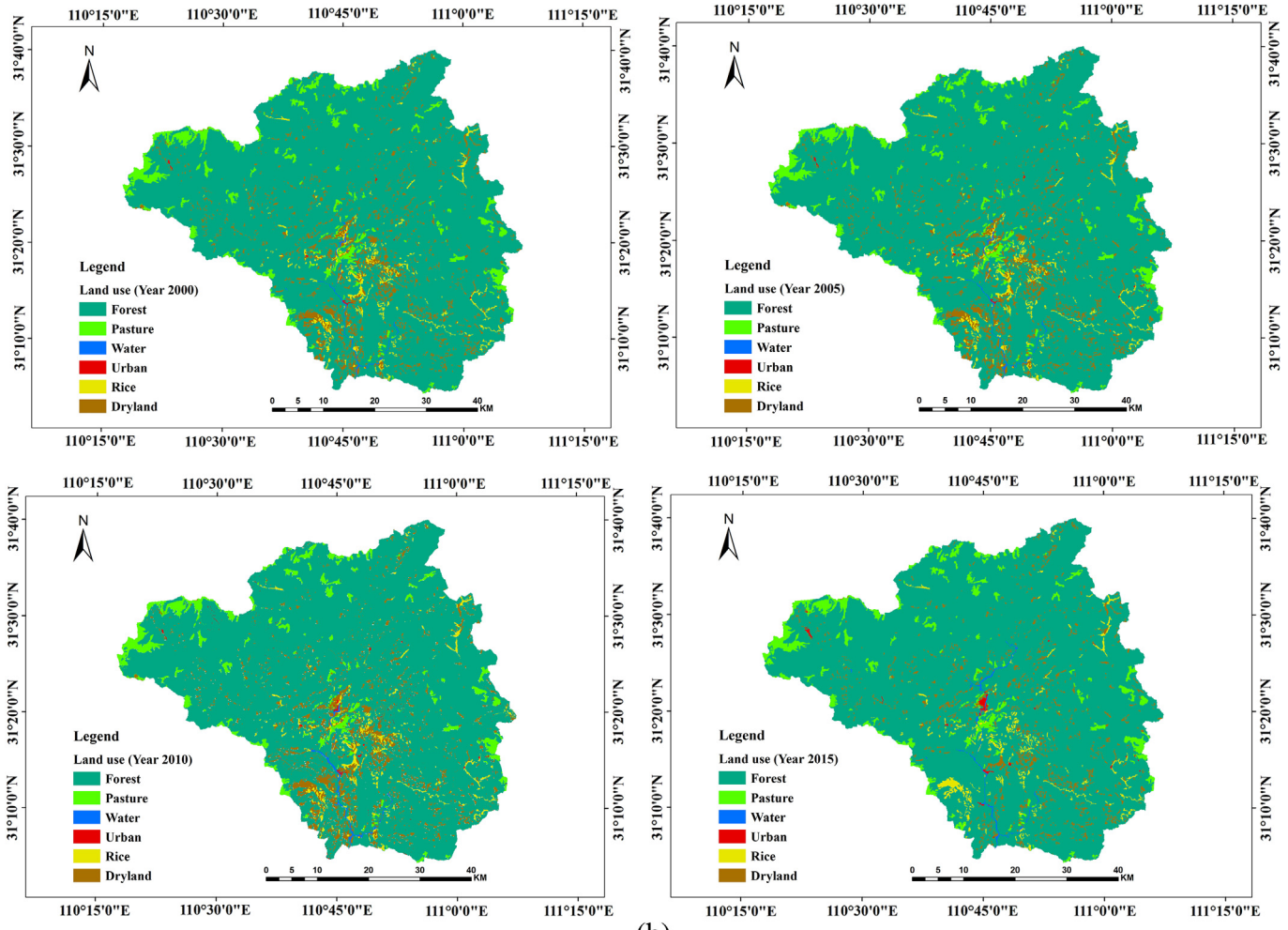

(b)

Fig. 2. Land use conversion from 2000 to 2015.

moisture content of soil on day i, R_{day} is the amount of rainfall on day i, Q_{surf} is the surface runoff on day i, E_a is the evapotranspiration amount on day i, W_{seep} is the water transferred from the soil profile into the gas zone on day i, and Q_{gw} is the return flow on day i.

The watershed will be divided into several subbasins in the SWAT model, using the hydrological analysis function in ArcGIS software based on DEM (Digital Elevation Model) data (Winchell et al., 2013). In each subbasin, Hydrological Response Units (HRUs) were defined based on a unique combination of land use, soil and slope data. Different inputs for these data will produce different definition of HRUs. Soil and

Table 1
The inconsistency index between different land use patterns (%).

	Land use 2000	Land use 2005	Land use 2010	Land use 2015
Land use 2000	0	1.08	4.87	14.17
Land use 2005	1.08	0	2.20	13.13
Land use 2010	4.87	2.20	0	12.85
Land use 2015	14.17	13.13	12.85	0

slope will not change greatly over a long time period, while land use may change frequently.

The SWAT Calibration and Uncertainty Programs (SWAT-CUP), a program developed for the sensitivity analysis, calibration, validation and uncertainty analysis of the SWAT model (Abbaspour, 2014), was used to calibrate the parameters in the SWAT model in this study. The Sequential Uncertainty Fitting version 2 (SUFI-2) algorithm in SWAT-CUP was selected as the calibration algorithm due to its good performance in large watersheds (Rostamian et al., 2008). The coefficient of determination (R^2) and Nash-Sutcliffe efficiency (NSE) were used to evaluate the performance of the SWAT model (Eqs. (2) and (3)).

$$R^2 = \frac{[\sum_{i=1}^{n}(O_i-\overline{O})(P_i-\overline{P})]^2}{\sum_{i=1}^{n}(O_i-\overline{O})^2\sum_{i=1}^{n}(P_i-\overline{P})^2} \quad (2)$$

$$NSE = \frac{\sum_{i=1}^{n}(O_i-\overline{O})^2-\sum_{i=1}^{n}(P_i-O_i)^2}{\sum(O_i-\overline{O})^2} \quad (3)$$

where $\overline{O}$ is the mean value of the observed values, O_i is the i^{th} observed value, P_i is the i^{th} simulated value, $\overline{P}$ is the mean value of the simulated values and n is the total count of the sample pairs.

2.3. Input data and model set up

Land use data for 2000, 2005, 2010 and 2015 were interpreted from the Landsat5 TM dataset with a resolution of 30 m. The DEM input was obtained from the second version of the Advanced Spaceborne Thermal Emission and Reflection Radiometer Global Digital Elevation Model dataset (http://www.gscloud.cn/). The soil input data were obtained from the Institute of Geography, Chinese Academy of Sciences, with a resolution of 30 m. The physical and chemical characteristics of the soil in the study area were obtained from the Chinese soil database and field survey. Weather input data from 2000 to 2016, including precipitation, temperature, relative humidity, solar radiation and wind data, were collected from the 9 weather stations in the watershed. The monitoring data of daily stream flow, total nitrogen (TN) and total phosphorus (TP) from 2004 to 2016 were obtained from the Yichang hydrographic office, Hubei Province, China.

In our research, the years 2000 and 2001 were used as the model warm-up period and those of 2002 to 2016 were used to analyze the impacts of land use inputs on the SWAT model. Seven land use input conditions were established, including four static conditions: just the land use in 2000 (JY2000), 2005 (JY2005), 2010 (JY2010) and 2015 (JY2015); and three dynamic conditions: those changing every 5 years (CE5Y), 10 years (CE10Y) and 15 years (CE15Y). The dynamic land use conditions were established by editing the lup.dat file in SWAT model, which was used by SWAT to consider the land use change during the simulation period. The spatial analysis and statistics function in ArcGIS was used to write the dynamic land use changes into the lup.dat file. Seven independent models were set up based on these seven different land use input conditions. The calibration and validation processes were carried out independently for each of the seven models, i.e., each model would have its own unique combination of parameters after calibrated.

2.4. Uncertainty analysis methods

The inconsistency index (IC) was used as the indicator to represent the degree of deviation between two land use patterns. The value was calculated based on the Kappa coefficient. Kappa coefficient is a method used to perform the consistency check, and it can be used to evaluate the differences between different land use maps (Yang et al., 2017b). The value of the Kappa coefficient ranges from −1 to 1; the higher the value is, the more consistent the land use maps are. The definition of the inconsistency index is (Eq. (4)):

$$\begin{aligned} IC &= (1-K)\times 100\% \\ K &= (P_0-P_e)/(1-P_e) \\ P_0 &= (s_1+s_2+\cdots+s_c)/n \\ P_e &= (s_1\times r_1+s_2\times r_2+\cdots+s_c\times r_c)/(n\times n) \end{aligned} \quad (4)$$

where K is the Kappa coefficient, P_0 is the total classification accuracy, P_e is the classification accuracy based on the confusion matrix, $s_1, s_2, \cdots, s_c$ are the simulated raster counts of each land use category, $r_1, r_2, \cdots, r_c$ are the actual raster counts of each land use category and n is the total raster counts of all land use categories.

The total inconsistency index (TIC) was used to quantify the deviation between the land use data used in the model and that in the real situation for the entire simulation period. In this study, the CE5Y condition was regarded as the real land use situation, because the land use would not change too much in every five years and due to the data limitation, this was the finest data we could obtain. The total inconsistency index was defined as follows (Eq. (5)):

$$TIC = \sum_{i=1}^{n} IC_i \quad (5)$$

where IC_i is the inconsistency index at the i^{th} node, i is the land use change node at which the land use change occurs, and n is the total count of the land use change nodes.

The uncertainty of the SWAT model outputs resulting from the different settings of land use input data was evaluated and quantified using several indicators: relative difference (RD), mean absolute difference (MAD) and root mean square deviation (RMSD). RD represented error percentage compared to the real data. The reliability of the predicted data could be evaluated by RD easily. MAD could represent the real condition of the error better with a quantitative value. RMSD could reflect the error between observed values and predicted values more obviously compared to MAD because the square was used to magnify the deviation. However, MAD and RMSD could be affected by the outliers easily, particularly for RMSD, while RD would not. The definition of the three indicators was listed as follows (Eqs. (6)–(8)):

$$RD = (P_i-S_i)/S_i \quad (6)$$

$$MAD = \frac{1}{n}\sum_{i=1}^{n}|P_i-S_i| \quad (7)$$

$$RMSD = \left[\frac{1}{n}\sum_{i=1}^{n}(P_i-S_i)^2\right]^{0.5} \quad (8)$$

where P_i is the predicted model output from the low changing frequency land use scenarios, S_i is the predicted model output from the CE5Y, which was used as a baseline for comparison with the outputs under other land use input scenarios, and n is the number of sample pairs.

3. Results

3.1. Land use change analysis

The forest area exhibited a downtrend from 2000 to 2010, with decreasing areas of approximately 31 ha and 205 ha from 2000 to 2005 and 2005 to 2010, respectively (Fig. 2a). The decreasing forest area was primarily converted into cultivated land. Different from 2000 to 2010,

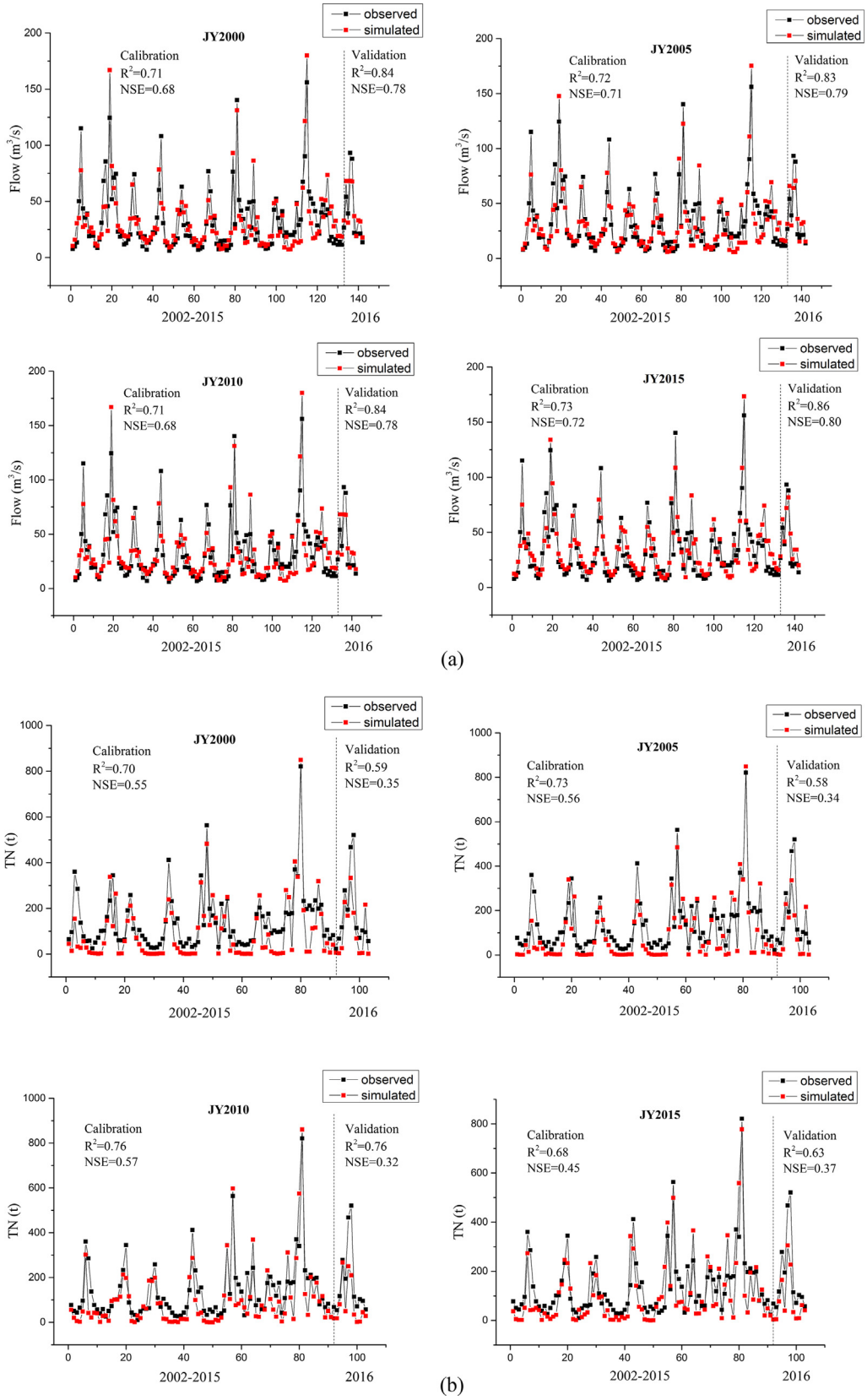

Fig. 3. Calibration and validation of flow, TN and TP under the static land use input conditions.

the forest area showed an uptrend from 2010 to 2015, and cultivated area decreased. The forest area increased by up to 1.9%, and the cultivated land area decreased by approximately 28.1%. Pasture, water and urban areas exhibited continuous increases from 2000 to 2015.

Spatially, there were no apparent differences between the land use patterns in 2000 and 2005 (Fig. 2b). In 2010, the increase in cultivated land area mainly occurred in the southern region of the watershed. The water area stretched to the northern area due to the impoundment of

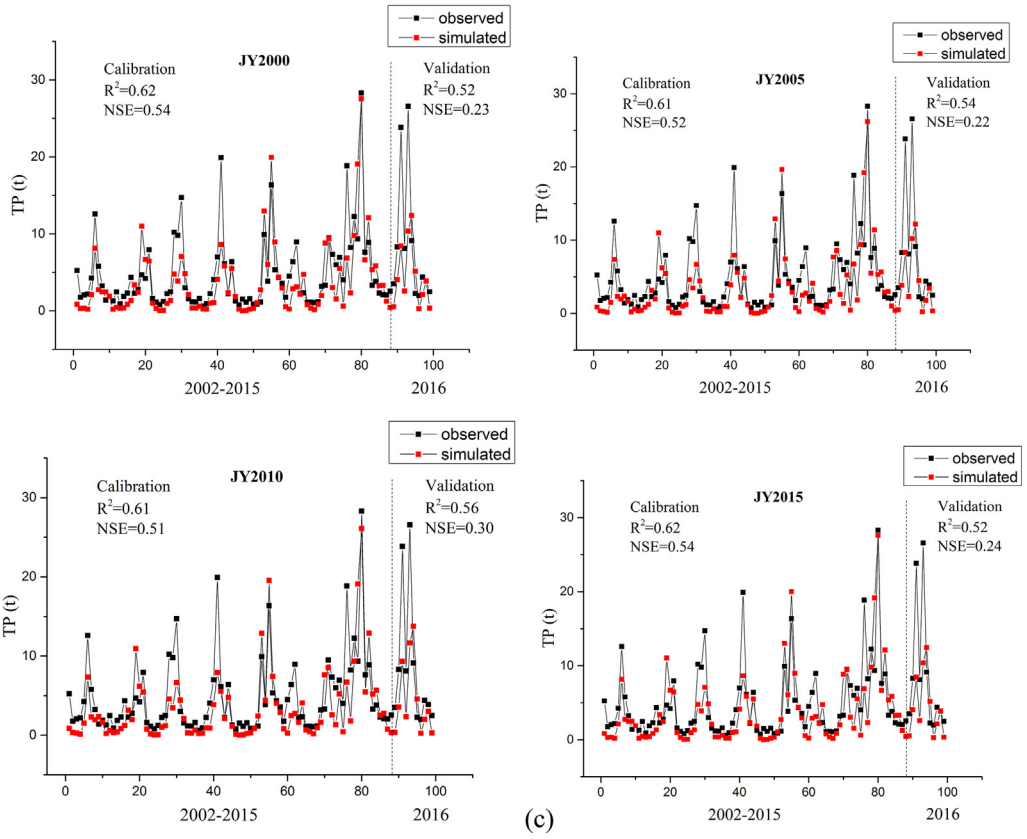

Fig. 3. (*continued*)

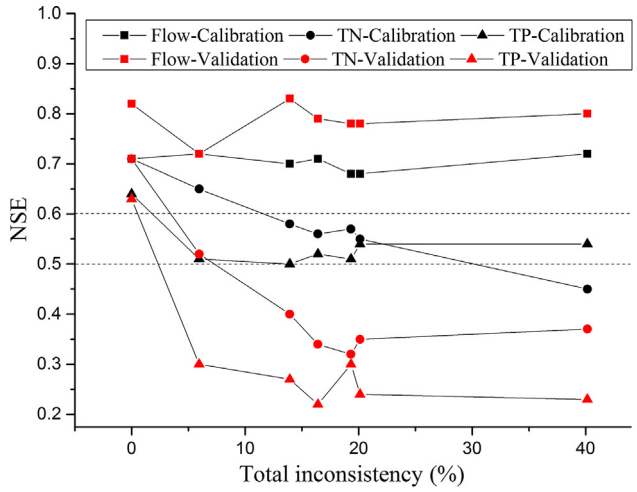

Fig. 4. Relationship between calibrated result and land use inconsistency index.

the Three Gorges Reservoir, and the expansion of urban areas occurred along the river. In 2015, the southwestern region of the watershed witnessed a decrease in cultivated land area, particularly in the drylands. The water area stretched further to the north of the watershed, and a large area of urban land appeared in the middle of the watershed.

The results of *IC* for each of the two land use patterns showed that the land use patterns in 2000 and 2005 had the highest consistency, with an *IC* of 1.08%, and the land use patterns in 2000 and 2015 had the lowest consistency, with an *IC* of 14.17% (Table 1). For different land use input conditions, the *TIC* values for the CE5Y, CE10Y, CE15Y, JY2000, JY2005, JY2010 and JY2015 conditions were 0%, 13.93%, 5.95%, 20.12%, 16.41%, 19.32% and 40.15%, respectively. The *TIC* was relatively lower under dynamic land use input conditions than it was under static land use input conditions.

3.2. Calibration and validation under static land use input conditions

For flow, the calibration and validation results showed no apparent differences under different land use input conditions (Fig. 3a). The R^2 and NSE coefficient were above 0.71 and 0.68, respectively, during the calibration periods. In addition, in the validation periods, the R^2 and NSE coefficient were even better than those in the calibration periods. For TN, the situation was quite different (Fig. 3b). The R^2 and NSE coefficient under the JY2005 and JY2010 conditions were better than those under the JY2000 and JY2015 conditions during the calibration periods. The NSE coefficient under the JY2015 condition even dropped below 0.50. Attention should be paid to the NSE coefficients during the validation periods because the NSE coefficients under all the conditions were quite low, with values only reaching approximately 0.35. For TP, the R^2 and NSE coefficient were similar under different conditions and were above 0.60 and 0.50, respectively, in the calibration periods (Fig. 3c). However, in the validation periods, the NSE coefficients were quite low, with values under 0.30.

Comparing the NSE to the *TIC* calculated previously, it could be found that the calibration and validation of flow had no evident relationship with the land use input condition (Fig. 4). However, for TN, the higher the *TIC* of the land use input was, the worse the calibration and validation results were. Similar to flow, the TP calibration was influenced little by the land use input conditions, while the NSE coefficient dropped dramatically to values below 0.3 when the *TIC* increased during the validation period.

3.3. Calibration and validation under dynamic land use input conditions

For flow, the R^2 and NSE coefficients were both above 0.70 during the entire calibration and validation periods (Fig. 5a). The calibration

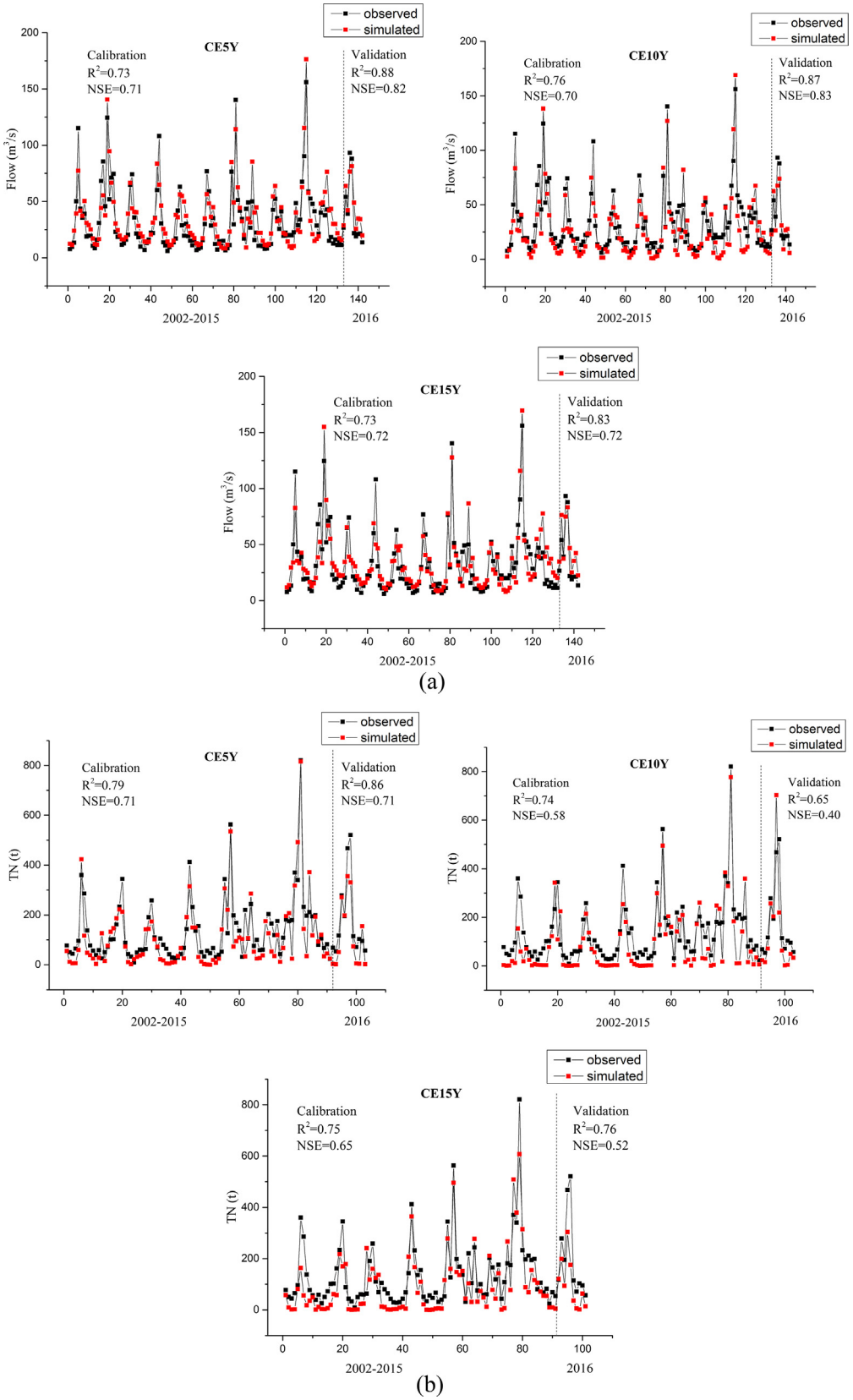

Fig. 5. Calibration and validation of flow, TN and TP under the dynamic land use input conditions.

and validation results had no apparent relationship with *TIC*. For TN, the calibrated results changed with changes in land use input conditions (Fig. 5b). The relationship between the *TIC* and the NSE coefficients was evident (Fig. 4). The higher the *TIC* was, the worse the NSE coefficient was for both calibration and validation periods. In the CE10Y scenario, with the highest *TIC* of the three dynamic conditions, the NSE coefficient was lower than 0.50 in the validation period. For TP, the R^2 and NSE coefficient reached the requirement of the SWAT

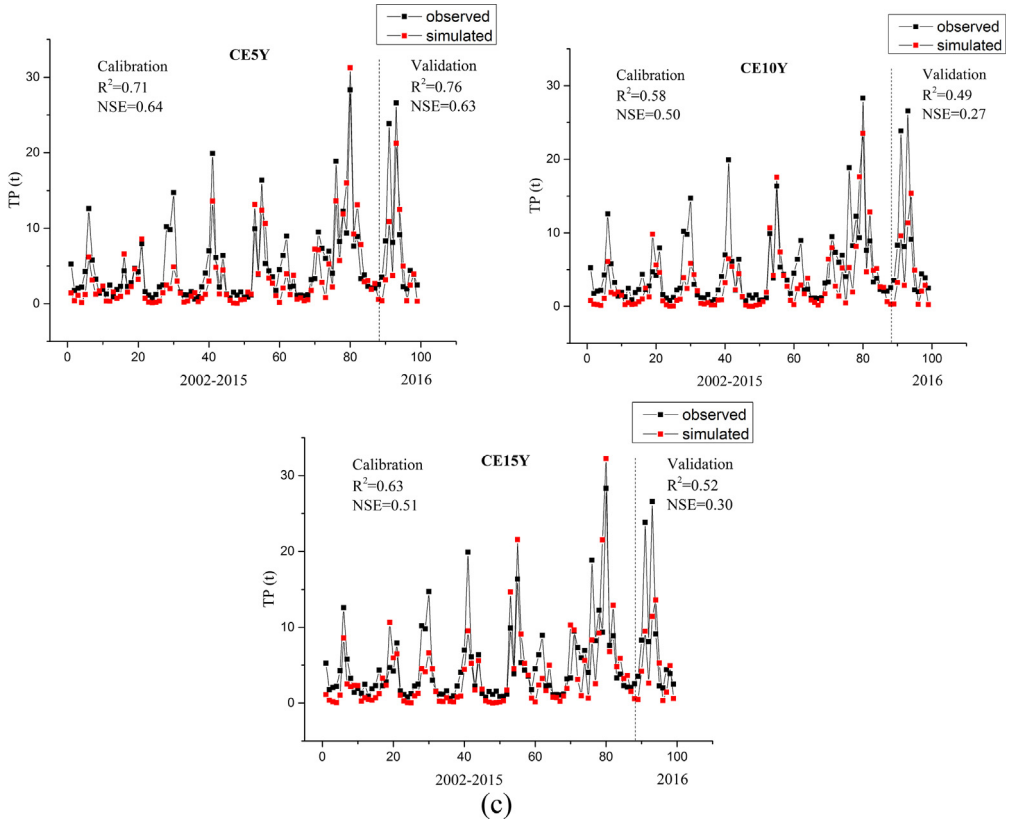

Fig. 5. (*continued*)

model accuracy, with values of higher than 0.5 in the calibration period under all three dynamic conditions (Fig. 5c). However, during the validation period, the calibrated results could satisfy the model's accuracy requirement only under the CE5Y condition.

Compared to the static conditions, the calibrated results for flow were similar to the R^2 and NSE coefficient, which were all approximately 0.7 during the calibration period and 0.8 during the validation period (Figs. 4a and 5a). However, for TN, it was better to use the dynamic land use input than the static land use input. The NSE coefficient increased from values of approximately 0.5 to 0.7 and from 0.3 to 0.5 during the calibration and validation periods, respectively (Figs. 4b and 5b). For TP, although the calibrated results reached the requirement of model accuracy under both the static and dynamic land use input conditions, during the calibration period, the NSE coefficients under dynamic land use input conditions were better than those under static land use input conditions during the validation period (Figs. 4c and 5c).

Among all seven land use input conditions, the results under the CE5Y condition showed the best performance, particularly for the TN and TP simulations. The NSE coefficient was 0.3 higher under the CE5Y condition than those under other land use input conditions during the validation period for TN. For TP, during the validation period, only the NSE coefficient under the CE5Y condition could reach the model's accuracy requirement, while the NSE coefficients under the other six land use input conditions were not higher than 0.3.

3.4. Uncertainty analysis of the SWAT model outputs

All of the model outputs under different land use input conditions were compared with those under the CE5Y condition to perform the uncertainty analysis. For annual outputs, the results showed that the uncertainties of the flow and TP outputs were relatively low, and the TN outputs had the highest uncertainty (Fig. 6). For flow, the RDs under different conditions were smaller than 10%, except under the JY2000 and JY2015 conditions, which had the highest *TIC* (Table 2). The JY2015 condition had the highest MAD and RMSD values, while the CE15Y condition had the lowest. For TN, the RD was only 1% under the CE15Y condition with a *TIC* of approximately 6%. However, with increasing *TIC*, the RDs increased to more than 10%. For TP, the RDs remained at approximately 3% under all conditions, and the MAD and RMSD values were also relatively low. However, it could be found that in the validation period (2016), a large difference existed for the TP outputs under different land use input conditions.

For the monthly outputs, the deviations were more obvious than those for annual outputs (Fig. 7). For flow, a sudden increase of the RDs occurred when the *TIC* reached 20% (Table 3). The JY2015 condition had the highest MAD and RMSD values of 238.80 and 270.70, respectively. For TN, under the static land use input conditions (JY2000, JY2005, JY2010 and JY2015), the RDs exceeded 20%, and the JY2015 condition had a dramatic 76% RD. For TP, the RDs under all land use input conditions reached 15%, except under the CE15Y condition.

The annual average monthly output and the monthly average deviation results were also analyzed, and the results indicated that deviation in outputs mainly occurred in the wet season, particularly for the TN and TP outputs (Fig. 8). For TN, the MAD values were 154.94 t, 64.76 t and 24.74 t in the wet, normal and dry seasons, respectively (Fig. 8b). The highest MAD occurred in June with a value of 82.87 t. The TN loads were apparently overestimated in the wet season under all land use input conditions, except under the JY2015 condition. For TP, the MAD values were 2.64 t, 0.62 t and 1.18 t in the wet, normal and dry seasons, respectively (Fig. 8c). The highest MAD occurred in August with a value of 1.56 t. Comparing TN with TP, the simulation of TP load under land use change conditions was less affected by changes in hydrological conditions caused by climate change than that of TN. The MAD value in the wet season was six times that in the dry season for TN and twice that for TP.

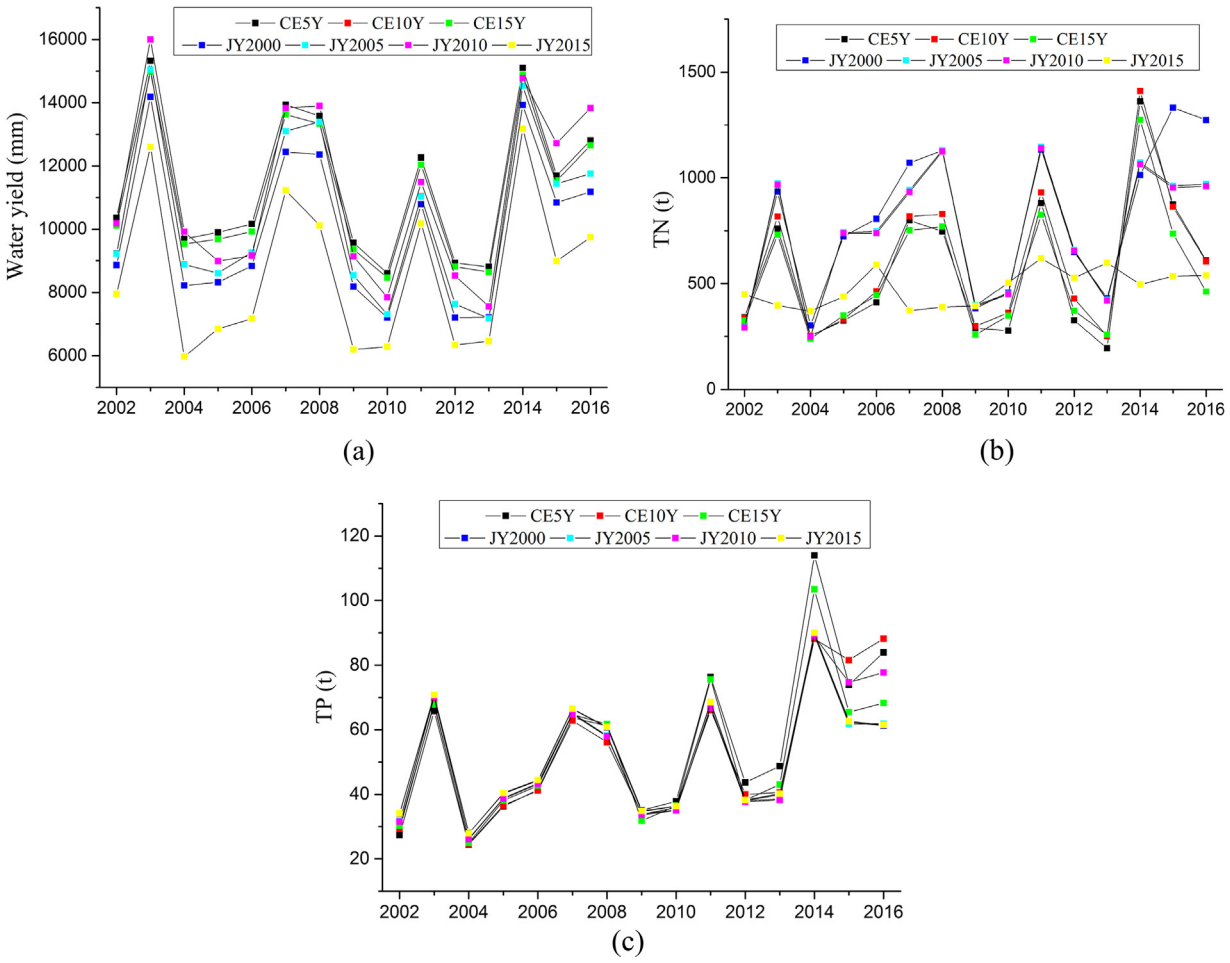

Fig. 6. Annual outputs of flow, TN and TP under different land use input conditions.

Table 2
Comparisons of annual flow, TN and TP loads under different land use input conditions with CE5Y.

Output	Indicator	CE10Y	CE15Y	JY2000	JY2005	JY2010	JY2015
Flow	RD	−0.09	−0.02	−0.13	−0.09	−0.02	−0.25
	MAD	920.08	212.17	1399.86	922.11	626.16	2765.93
	RMSD	1009.88	220.42	1416.58	1011.73	719.92	2810.41
TN	RD	0.09	0.01	0.55	0.46	0.45	0.17
	MAD	139.29	55.04	285.15	226.30	221.82	275.93
	RMSD	151.45	68.19	327.64	258.64	254.27	338.21
TP	RD	−0.03	−0.03	−0.03	−0.05	−0.03	−0.03
	MAD	4.95	4.08	7.19	7.16	5.38	7.13
	RMSD	8.05	5.90	10.08	10.11	8.04	9.97

4. Discussion

The calibrated results of flow indicated that both the static and dynamic land use inputs could be used to obtain an acceptable calibration and validation results. The results had no apparent relationship with the *TIC* (Fig. 4). This may be explained by the fact that land use is not the only decisive factor affecting runoff processes. Runoff processes are mainly driven by precipitation processes (Zhang et al., 2018) and are affected by several factors, such as soil moisture content, groundwater characteristics and channel properties (Ruggenthaler et al., 2015; House et al., 2016; Lu et al., 2016). Thus, when carrying out a simulation of the flow generation in a watershed, both the dynamic and static land use input approaches can be used. However, for TN, the calibration and validation results from the dynamic land use input conditions were clearly better than those from the static land use input conditions. When the *TIC* was below 10%, the NSE coefficient reached values above 0.60 and 0.50 during calibration and validation periods, respectively, which represented a good calibrated result (Abbaspour, 2014). In addition, when the *TIC* index was less than 20%, the NSE coefficient could reach values above 0.50 during the calibration period, representing an acceptable calibrated result. The results indicated that land use input conditions had a significant effect on the NPS nitrogen simulation. This was reasonable because NPS nitrogen pollutants were mainly derived from cultivated land (Ouyang et al., 2013), which changed with the conversion of land use patterns. It should be noted that under the static conditions, although the R^2 and NSE coefficients were above 0.50 during the calibration period, they were all below 0.50 during the validation periods. Thus, if a simulation which has a time period longer than calibration period was required, a land use input with a low *TIC* was needed, i.e., dynamic land use inputs were better. For TP, the similar calibrated results under different land use input conditions during the calibration periods indicated that the calibration process of TP was more affected by non-unique parameters. Several parameter sets with different values may provide equally suitable model responses (Beven, 1996), and due to the large amount of parameters participating in the TP calibration process, this phenomenon is more significant (Mehdi et al., 2017). However, only when the *TIC* was less than 5%, could the NSE coefficient reach 0.60. Moreover, during the validation periods, the NSE coefficients could reach 0.50 only under the CE5Y condition. Thus, land use patterns clearly have important effects on the simulation of phosphorus load (Wang et al., 2015). Through the perspective of calibration and validation results, it could be found that different land use input conditions did have great

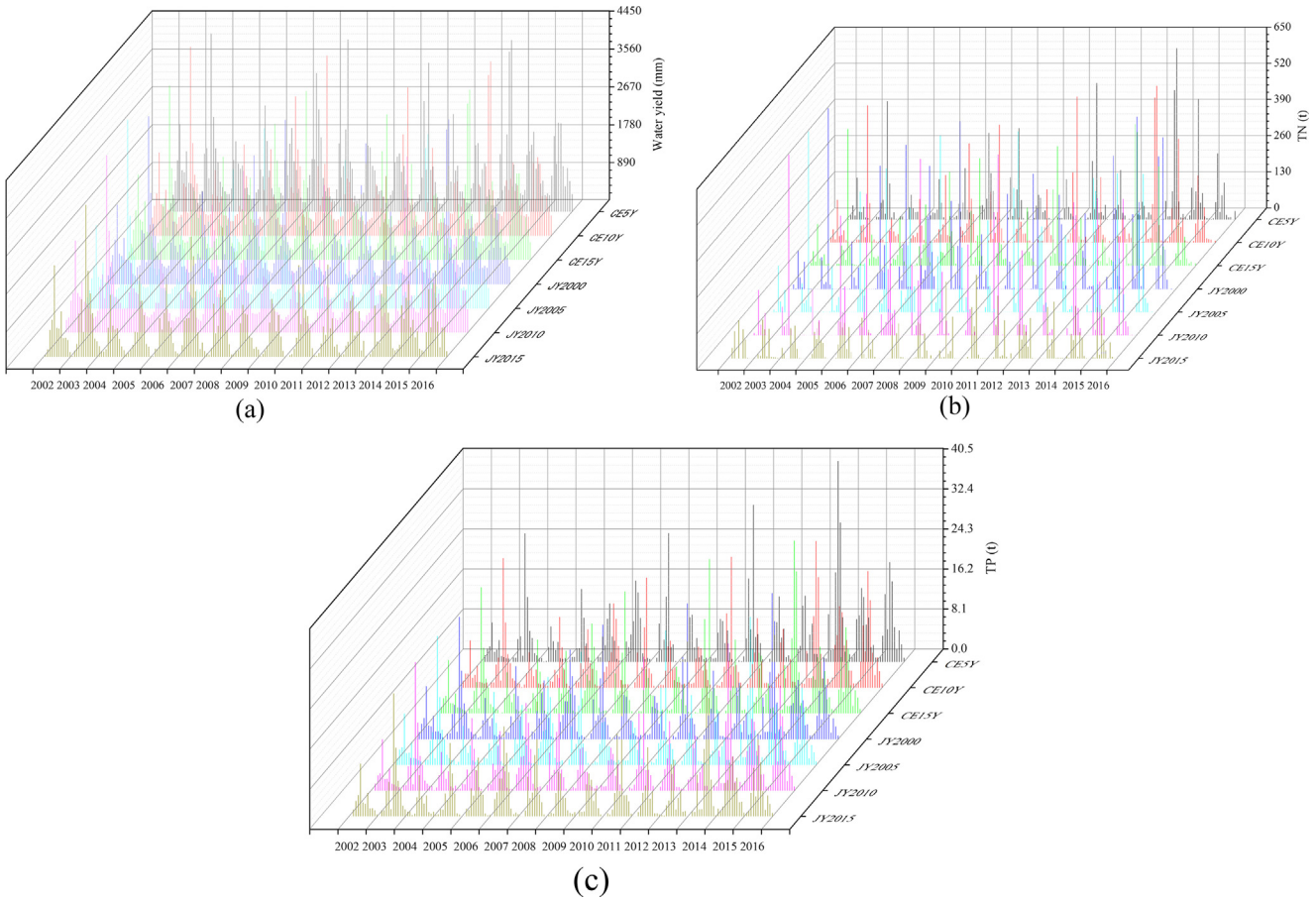

Fig. 7. Monthly outputs of flow, TN and TP under different land use input conditions.

Table 3
Comparisons of monthly flow, TN, TP loads under different land use input conditions with CE5Y.

Output	Indicator	CE10Y	CE15Y	JY2000	JY2005	JY2010	JY2015
Flow	RD	−0.04	−0.01	−0.12	−0.04	0.06	−0.36
	MAD	117.08	18.96	119.07	117.20	132.37	238.80
	RMSD	152.16	26.24	157.59	152.33	171.23	270.70
TN	RD	0.11	−0.05	0.26	0.21	0.20	0.76
	MAD	27.52	10.61	44.12	42.24	41.85	50.87
	RMSD	16.31	21.52	102.92	96.09	95.17	102.70
TP	RD	0.16	0.02	0.26	0.16	0.18	0.26
	MAD	0.56	0.59	0.78	0.74	0.62	0.77
	RMSD	1.27	1.01	1.46	1.42	1.25	1.44

importance on the model accuracy, and dynamic land use inputs could effectively improve the model performance, particularly for the nitrogen and phosphorus simulation.

The uncertainty analysis of the SWAT model outputs indicated that monthly outputs had greater uncertainty than annual outputs. The deviations were offset when calculating annual outputs. Thus, annual simulations required lower land use input accuracy than monthly simulations. For flow, although the influence of land use input conditions on the simulation results was not evident, monthly outputs would fluctuate when the land use change reached a relatively large level. For TN, under the JY2015 condition, which had the highest *TIC*, the RD value of annual outputs was relatively lower than those under other static land use input scenarios. However, it had the worst simulation performance, with the lowest NSE coefficient and monthly RD, MAD and RMSD values. This may be caused by its average annual output values, which offset the deviation on the whole (Fig. 6b). Thus, when evaluating the uncertainty of the outputs, multiple indicators were required (Wechsler, 2006). The deviation in TP outputs mainly occurred in 2016, i.e., during the validation periods, which again shows that land use input conditions have significant impacts on the simulation of TP load, although the calibrated results were excellent. The higher deviation of the TN and TP outputs in the wet seasons may have been caused by high-intensity rainfall during these months. High-intensity rainfall will lead to high surface runoff and will enhance water and soil erosion (Sadeghi et al., 2016). In addition, the NPS pollution discharge will simultaneously increase, leading to an increase in deviation (Ning et al., 2006).

Land use data were an important input for most of the hydrological and water quality models, which have a significant impact on the model outputs (Liu et al., 2017a). The land use pattern changed with time due to the impacts of climate change and human activities (Shi and Shiwenjiao, 2015). The precipitation and temperature change, construction of the Three Gorges Dam and the regulation put forward by the government to return farmland to forestland for ecological protection have greatly changed the land use pattern in the Three Gorges Reservoir area (Yao et al., 2017; Zhang et al., 2017). The impacts of climate change and human activities on land use changes have attracted extensive attention worldwide (Li et al., 2014; Gong et al., 2017). However, in most of the related studies, only one year of land use input data were used in the models, without considering the variations in land use throughout the entire simulation period (Awotwi et al., 2015; Samad et al., 2016). As land use patterns changed over different time periods, considering land use changes during the NPS simulation periods is of great importance.

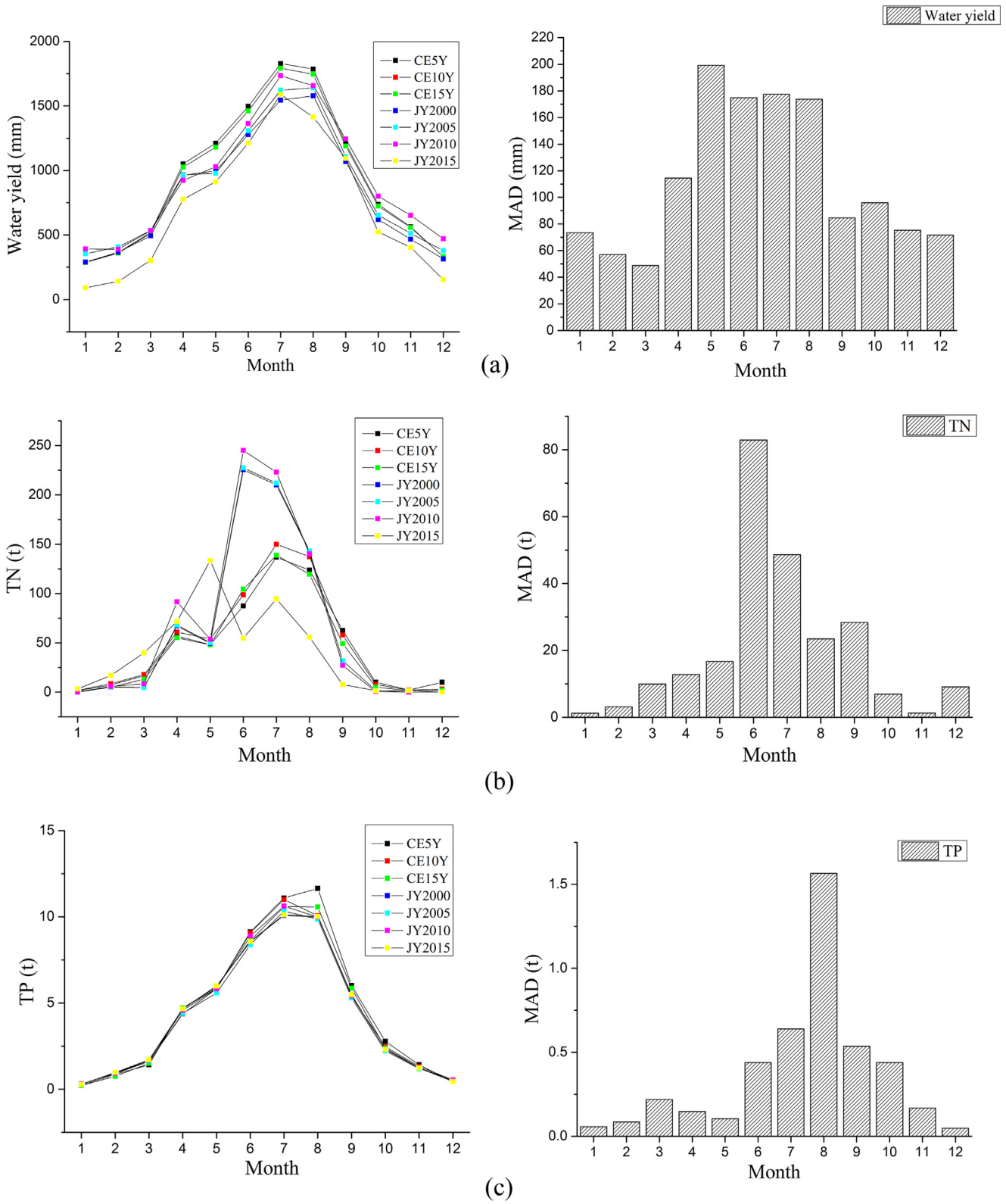

Fig. 8. Temporal variation of monthly outputs.

5. Conclusions

Land use patterns changed significantly from 2000 to 2015 in the Xiangxi River watershed. These changes mainly occurred between forest and cultivated areas. Forest area was continuously converted to cultivated area from 2000 to 2010, while approximately 28% of cultivated areas was converted to forest from 2010 to 2015. These changes were mainly caused by climate change and human activities.

To reveal the impacts of land use input conditions on the model performance, calibration and validation were carried out under seven different land use input conditions, including static and dynamic land use input approaches. The results indicated that, on the whole, dynamic

land use inputs could provide a better model performance than static land use inputs. Thus, if sufficient land use data are available, using the dynamic land use input is the best choice. The impacts of land use input conditions on the different simulated elements were different for annual outputs. Land use input data had relatively low impacts on the flow simulation. Thus, when simulating the flow or water yield in a watershed, the land use in any year during the simulation period can be selected as the input. For TN, the simulation accuracy decreased when the *TIC* increased. For TP, it is suggested that land use input data with a lower *TIC* should be used. This is because although the calibration effects were satisfactory during the calibration periods, only the land use input data with low *TIC* reached the requirements of the model's accuracy during the validation period. Moreover, if monthly outputs are required from the model, a dynamic land use input with low *TIC* is necessary because land use conditions have a greater impact on model monthly outputs than on annual outputs, particularly in the wet seasons.

In this study, the impacts of land use change on the model performance was studied based on the calibrated results and uncertainty analysis of the model outputs. The significance of using dynamic land use input instead of static land use input when simulating NPS contamination in a watershed within a long time series using models was revealed. This study could provide support for setting the land use input condition when using other NPS models in other areas.

Acknowledgments

This study was funded by the National Key Research and Development Program of China (2017YFA0605001), the National Natural Science Foundation of China (41571486) and the Interdisciplinary Research Funds of Beijing Normal University. The authors thank the editors and anonymous reviewers for their valuable comments and suggestions.

References

Abbaspour, K., 2014. SWAT-CUP 2012: SWAT Calibration and Uncertainty Programs—A User Manual. Swiss Federal Institute of Aquatic Science and Technology, Switzerland.
Ahn, S.-R., Kim, S.-J., 2016. The effect of rice straw mulching and no-tillage practice in upland crop areas on nonpoint-source pollution loads Based on HSPF. Water 8 (3).
Arnold, J.G., Srinivasan, R., Muttiah, R.S., Williams, J.R., 1998. Large area hydrologic modeling and assessment – part 1: model development. J. Am. Water Resour. Assoc. 34 (1), 73–89.
Arnold, J.G., Williams, J.R., 1987. Validation of SWRRB – simulator for water-resources in rural basins. J. Water Resour. Plann. Manag. ASCE 113 (2), 243–256.
Arnold, J.G., Williams, J.R., Maidment, D.R., 1995. Continuous-time water and sediment routing model for large basins. J. Hydraul. Eng. ASCE 121 (2), 171–183.
Awotwi, A., Yeboah, F., Kumi, M., 2015. Assessing the impact of land cover changes on water balance components of White Volta Basin in West Africa. Water Environ. J. 29 (2), 259–267.
Bajracharya, A.R., Bajracharya, S.R., Shrestha, A.B., Maharjan, S.B., 2018. Climate change impact assessment on the hydrological regime of the Kaligandaki Basin, Nepal. Sci. Total Environ. 625, 837–848.
Beven, K., 1996. The limits of splitting: hydrology. Sci. Total Environ. 183 (1–2), 89–97.
Chen, L., Sun, C., Wang, G., Xie, H., Shen, Z., 2017. Event-based nonpoint source pollution prediction in a scarce data catchment. J. Hydrol. 552.
Chen, Y., Cheng, S., Liu, L., Guo, X., Wang, Z., Qin, C., Hao, R., Lu, J., Gao, J., 2013. Assessing the effects of land use changes on non-point source pollution reduction for the Three Gorges Watershed using the SWAT model. J. Environ. Inf.
Chu, H.-J., Lin, Y.-P., Huang, C.-W., Hsu, C.-Y., Chen, H.-Y., 2010. Modelling the hydrologic effects of dynamic land-use change using a distributed hydrologic model and a spatial land-use allocation model. Hydrol. Process. 24 (18), 2538–2554.
Du, X., Su, J., Li, X., Zhang, W., 2016. Modeling and evaluating of non-point source pollution in a semi-arid watershed: implications for watershed management. Clean-Soil Air Water 44 (3), 247–255.
Gashaw, T., Tulu, T., Argaw, M., Worqlul, A.W., 2018. Modeling the hydrological impacts of land use/land cover changes in the Andassa watershed, Blue Nile Basin, Ethiopia. Sci. Total Environ. 619, 1394–1408.
Gong, J., Zhang, J., Qian, C., Ma, X., Liu, D., 2017. Response of land use change on human activities in Bailongjiang watershed of Gansu Province During 1990–2014. Bull. Soil Water Conserv. 37 (4), 219–224.
Goyal, M.K., Panchariya, V.K., Sharma, A., Singh, V., 2018. Comparative assessment of SWAT model performance in two distinct catchments under various DEM scenarios of varying resolution, sources and resampling methods. Water Resour. Manage. 32 (2), 805–825.
House, A.R., Thompson, J.R., Sorensen, J.P.R., Roberts, C., Acreman, M.C., 2016. Modelling groundwater/surface water interaction in a managed riparian chalk valley wetland. Hydrol. Process. 30 (3), 447–462.
Kang, M.S., Park, S.W., Lee, J.J., Yoo, K.H., 2006. Applying SWAT for TMDL programs to a small watershed containing rice paddy fields. Agric. Water Manage. 79 (1), 72–92.
Karki, R., Tagert, M.L.M., Paz, J.O., Bingner, R.L., 2017. Application of AnnAGNPS to model an agricultural watershed in East-Central Mississippi for the evaluation of an on-farm water storage (OFWS) system. Agric. Water Manag. 192, 103–114.
Kumar, B., Lakshmi, V., Patra, K.C., 2017. Evaluating the uncertainties in the SWAT Model outputs due to DEM grid size and resampling techniques in a Large Himalayan River Basin. J. Hydrol. Eng. 22 (9).
Li, Z., Li, X., Tang, J., Liu, C., Wang, X., 2014. Study on the response of land use/land cover to climate change in Liao River Basin of Jilin Province. Res. Soil Water Conserv. 21 (6), 104–110.
Lin, C., Ma, R., Xiong, J., 2018. Can the watershed non-point phosphorus pollution be interpreted by critical soil properties? A new insight of different soil P states. Sci. Total Environ. 628–629, 870–881.
Liu, J., Zhang, C., Kou, L., Zhou, Q., 2017a. Effects of climate and land use changes on water resources in the Taoer River. Advances in Meteorology.
Liu, M., Li, C., Hu, Y., Sun, F., Xu, Y., Chen, T., 2014. Combining CLUE-S and SWAT models to forecast land use change and non-point source pollution impact at a watershed scale in Liaoning Province, China. Chin. Geog. Sci. 24 (5), 540–550.
Liu, R., Wang, Q., Xu, F., Men, C., Guo, L., 2017b. Impacts of manure application on SWAT model outputs in the Xiangxi River watershed. J. Hydrol. 555, 479–488.
Liu, R., Xu, F., Zhang, P., Yu, W., Men, C., 2016. Identifying non-point source critical source areas based on multi-factors at a basin scale with SWAT. J. Hydrol. 533, 379–388.
Liu, R., Zhang, P., Wang, X., Chen, Y., Shen, Z., 2013. Assessment of effects of best management practices on agricultural non-point source pollution in Xiangxi River watershed. Agric. Water Manag. 117, 9–18.
Lu, S., Zhang, L., Guo, S., Fan, L., Meng, J., Wang, G., 2016. Forty years' channel change on the Yongdinghe River, China: patterns and causes. Int. J. River Basin Manage. 14 (2), 183–193.
Mehdi, B., Schulz, K., Ludwig, R., Ferber, F., Lehner, B., 2017. Evaluating the importance of non-unique behavioural parameter sets on surface water quality variables under climate change conditions in a mesoscale agricultural watershed. Water Resour. Manage. 4, 1–21.
Mi, Y., He, C., Bian, H., Cai, Y., Sheng, L., Ma, L., 2015. Ecological engineering restoration of a non-point source polluted river in Northern China. Ecol. Eng. 76, 142–150.
Minta, M., Kibret, K., Thorne, P., Nigussie, T., Nigatu, L., 2018. Land use and land cover dynamics in Dendi-Jeldu hilly-mountainous areas in the central Ethiopian highlands. Geoderma 314, 27–36.
Moges, M.A., Schmitter, P., Tilahun, S.A., Steenhuis, T.S., 2017. Watershed modeling for reducing future non-point source sediment and phosphorus load in the Lake Tana Basin, Ethiopia. J. Soils Sediments 10, 1–14.
Ning, S.K., Chang, N.B., Jeng, K.Y., Tseng, Y.H., 2006. Soil erosion and non-point source pollution impacts assessment with the aid of multi-temporal remote sensing images. J. Environ. Manage. 79 (1), 88–101.
Ouyang, W., Huang, H., Hao, F., Guo, B., 2013. Synergistic impacts of land-use change and soil property variation on non-point source nitrogen pollution in a freeze-thaw area. J. Hydrol. 495, 126–134.
Ouyang, W., Jiao, W., Li, X., Giubilato, E., Critto, A., 2016. Long-term agricultural non-point source pollution loading dynamics and correlation with outlet sediment geochemistry. J. Hydrol. 540, 379–385.
Ouyang, W., Song, K., Wang, X., Hao, F., 2014. Non-point source pollution dynamics under long-term agricultural development and relationship with landscape dynamics. Ecol. Ind. 45 (5), 579–589.
Rostamian, R., Jaleh, A., Afyuni, M., Mousavi, S.F., Heidarpour, M., Jalalian, A., Abbaspour, K.C., 2008. Application of a SWAT model for estimating runoff and sediment in two mountainous basins in central Iran. Hydrol. Sci. J. 53 (5), 977–988.
Ruggenthaler, R., Schoeberl, F., Markart, G., Klebinder, K., Hammerle, A., Leitinger, G., 2015. Quantification of Soil Moisture Effects on Runoff Formation at the Hillslope Scale. J. Irrig. Drain. Eng. 141 (9).
Sadeghi, S.H.R., Moghadam, E.S., Darvishan, A.K., 2016. Effects of subsequent rainfall events on runoff and soil erosion components from small plots treated by vinasse. CATENA 138, 1–12.
Samad, N., Chauhdry, M.H., Ashraf, M., Saleem, M., Hamid, Q., Babar, U., Tariq, H., Farid, M.S., 2016. Sediment yield assessment and identification of check dam sites for Rawal Dam catchment. Arabian J. Geosci. 9 (6).
Sewnet, A., Abebe, G., 2017. Land use and land cover change and implication to watershed degradation by using GIS and remote sensing in the Koga watershed, North Western Ethiopia. Earth Sci. Inf. 1–10.
Shen, Z., Zhong, Y., Huang, Q., Chen, L., 2015. Identifying non-point source priority management areas in watersheds with multiple functional zones. Water Res. 68, 563–571.
Shi, X., Shiwenjiao, 2015. Identifying contributions of climate change and human activities to spatial-temporal cropland changes: a review. Acta Geog. Sin. 70 (9), 1463–1476.
Sun, J., Li, Y.P., Huang, G.H., Wang, C.X., 2017. Analysis of interactive effects of DEM resolution and basin subdivision level on runoff simulation in Kaidu River Basin, China. Hydrol. Res. 48 (4), 1100–1117.
Teshager, A.D., Gassman, P.W., Secchi, S., Schoof, J.T., 2017. Simulation of targeted pollutant-mitigation-strategies to reduce nitrate and sediment hotspots in agricultural watershed. Sci. Total Environ. 607–608, 1188–1200.
Wagner, P.D., Bhallamudi, S.M., Narasimhan, B., Kumar, S., Fohrer, N., Fiener, P., 2017. Comparing the effects of dynamic versus static representations of land use change in

hydrologic impact assessments. Environ. Modell. Software.
Wang, J., Shao, J.A., Wang, D., Ni, J., Xie, D., 2015. Simulation of the dissolved nitrogen and phosphorus loads in different land uses in the Three Gorges Reservoir Region-based on the improved export coefficient model. Environ. Sci. Process. Impacts 17 (11), 1976–1989.
Wang, X., Zhang, W., Huang, Y., Li, S., 2004. Modeling and simulation of point-non-point source effluent trading in Taihu Lake area: perspective of non-point sources control in China. Sci. Total Environ. 325 (1–3), 39–50.
Wechsler, S.P., 2006. Uncertainties associated with digital elevation models for hydrologic applications: a review. Hydrol. Earth Syst. Sci. Discuss. 3 (4), 1481–1500.
Winchell, M., Srinivasan, R., Di Luzio, M., Arnold, J., 2013. ArcSWAT Interface for SWAT 2012. User's Guide. Blackland Research and Extension Center.
Worku, T., Khare, D., Tripathi, S.K., 2017. Modeling runoff-sediment response to land use/land cover changes using integrated GIS and SWAT model in the Beressa watershed. Environ. Earth Sci. 76 (16).
Yang, B., Huang, K., Sun, D., Zhang, Y., 2017a. Mapping the scientific research on non-point source pollution: a bibliometric analysis. Environ. Sci. Pollut. Res. 24 (5), 4352–4366.
Yang, C., Wu, G., Ding, K., Shi, T., Li, Q., Wang, J., 2017b. Improving land use/land cover classification by integrating pixel unmixing and decision tree methods. Remote Sensing 9 (12), 1222.
Yang, X., Tan, L., He, R., Fu, G., Ye, J., Liu, Q., Wang, G., 2017c. Stochastic sensitivity analysis of nitrogen pollution to climate change in a river basin with complex pollution sources. Environ. Sci. Pollut. Res. 24 (34), 26545–26561.
Yao, Y.-S., Wang, Q.-L., Liao, W.-L., Zhang, L.-F., Chen, J.-H., Li, J.-G., Yuan, L., Zhao, Y.-N., 2017. Influences of the Three Gorges Project on seismic activities in the reservoir area. Sci. Bull. 62 (15), 1089–1098.
Zhai, X., Zhang, Y., Wang, X., Xia, J., Liang, T., 2014. Non-point source pollution modelling using Soil and Water Assessment Tool and its parameter sensitivity analysis in Xin'anjiang catchment, China. Hydrol. Process. 28 (4), 1627–1640.
Zhang, P., Liu, Y.H., Pan, Y., Yu, Z.R., 2013. Land use pattern optimization based on CLUE-S and SWAT models for agricultural non-point source pollution control. Math. Comput. Modell. 58 (3–4), 588–595.
Zhang, X., Li, P., Li, Z.B., Yu, G.Q., Li, C., 2018. Effects of precipitation and different distributions of grass strips on runoff and sediment in the loess convex Hillslope. CATENA 162, 130–140.
Zhang, Y., Zhong, P.-A., Chen, J., Bing, J., Xu, D., Wang, M., 2017. Impacts of Climate Change and Human Activities on the Three Gorges Reservoir Inflow. Water 9 (12).
Zhi, X., Chen, L., Shen, Z., 2018. Impacts of urbanization on regional nonpoint source pollution: case study for Beijing, China. Environ. Sci. Pollut. Res. Int.